TurboSENSE: Phase Estimation in Temporal Phase-Constrained Parallel Imaging

C. Lew[1], D. Spielman[1], R. Bammer[1]

[1]Stanford University, Stanford, CA, United States

Introduction: SENSE(1) has been shown to reduce the acquisition time or to minimize the level of distortion of an image. Often, only the magnitude of an image is of importance. Previous work (2, 3), so called phase-constrained GEM or turboSENSE, separates the real and imaginary channels to double the number of equations in the general SENSE formulation. The phase of the image is then estimated and incorporated into the SENSE matrix, which effectively rotates the image into real space. A modified g-factor can be calculated that depends upon the noise from the real and imaginary channels. The resulting image has been shown to have a lower g-factor than conventional SENSE at the same reduction factor. This abstract investigates the performance of SENSE to turboSENSE at comparable number of phase encodes.

Theory: Multi-phase applications, such as diffusion-weighted imaging and fMRI, require repeated acquisition of an imaging slice. In applications that SENSE reduces acquisition time, the number of phase encodes is reduced by a factor R. Although turboSENSE can reduce the number of phase encodes further, it needs an accurate phase estimate per pass. If a low-resolution phase estimate is collected at each pass, the total number of phase encodes from the low-resolution phase estimate and from the turboSENSE acquisition must be less than the phase encodes for the conventional SENSE acquisition for there to be a net speedup. The turboSENSE matrix can be expressed as the sum of a perfect matrix **A** and perturbation matrix **E**. **A** represents the encoding coil sensitivity $|\mathbf{C}|\exp(i\angle\mathbf{C})$ with the perfect phase estimate of the image $\exp(i\boldsymbol{\varphi})$ separated into real and imaginary parts. **E** represents the deviation from the perfect phase estimate with $\boldsymbol{\varphi} + \boldsymbol{\varepsilon} = \boldsymbol{\varphi}'$, where $\boldsymbol{\varepsilon}$ denotes the phase error and $\boldsymbol{\varphi}'$ is the phase estimate. The matrix equation can be written as Eq. 1, where **x** represents the pixel intensity, $\boldsymbol{\delta}\mathbf{x}$ represents the reconstruction error, and **b** is the measured aliased pixel intensity values separated into real and imaginary parts. The error depends on coil sensitivity with sinusoidal weights in the real and imaginary channels. Ignoring the noise in the measured data, it is known (4) that the reconstruction error has an upper bound that depends on the condition number κ, the error matrix norm ||**E**||, and the matrix norm of ||**A**|| (see Eq. 2).

$$(\mathbf{A}+\mathbf{E})(\mathbf{x}+\delta\mathbf{x})=\mathbf{l} \quad \text{Eq. 1}$$

$$\mathbf{A}=\begin{bmatrix}\mathrm{Re}(|\mathbf{C}|e^{i\angle\mathbf{C}}e^{i\varphi})\\ \mathrm{Im}(|\mathbf{C}|e^{i\angle\mathbf{C}}e^{i\varphi})\end{bmatrix}$$

$$\mathbf{E}=\begin{bmatrix}\mathrm{Re}(|\mathbf{C}|e^{i\angle\mathbf{C}}e^{i\varphi}(e^{i\varepsilon}-1))\\ \mathrm{Im}(|\mathbf{C}|e^{i\angle\mathbf{C}}e^{i\varphi}(e^{i\varepsilon}-1))\end{bmatrix}$$

$$\frac{\|\delta\mathbf{x}\|}{\|\mathbf{x}\|}\le\frac{\kappa\frac{\|\mathbf{E}\|}{\|\mathbf{A}\|}}{1-\kappa\frac{\|\mathbf{E}\|}{\|\mathbf{A}\|}},\ \text{for}\ \kappa\frac{\|\mathbf{E}\|}{\|\mathbf{A}\|}<1 \quad \text{Eq. 2}$$

Methods: The SENSE and turboSENSE acquisitions were simulated with fully-sampled *in-vivo* T2-weighted images from a GE Signa 1.5T scanner. Data was acquired with a fast spin echo Cartesian sequence, a 256x256 matrix, and an echo train length of 8. Gaussian noise with a variance of 10% of the maximum intensity was added. In addition, coil sensitivity noise that is 1% of the maximum sensitivity was added. Coil sensitivities from a 4-coil circular array were used with a simulated Gaussian-shaped sensitivity distribution. The coil plane was perpendicular to the image plane, and the coils were placed 90 degrees apart. The coil sensitivities were masked by the original image at the noise level. The k-space data was undersampled and Fourier transformed to image space. SENSE or turboSENSE reconstruction was performed on each set of aliased pixels using singular value decomposition. The number of aliased pixels to be reconstructed was further reduced by the threshold mask. g-factor maps were calculated. Let λ be the fraction of the full resolution image used for the phase estimate. The central 256*λ k-space lines were kept, and the matrix was zero-padded to 256 phase encodes before being Fourier transformed to obtain the phase estimate. Comparable number of phase encodes were simulated for test 1 [SENSE (R=3) and turboSENSE (R=4, λ=1/8)] and for test 2 [SENSE (R=4) and turboSENSE (R=5,λ=1/16)]. turboSENSE for the set {(R=4,λ=1/32), (R=5,λ=1/32), (R=5,λ=1/2)} were also simulated. The matrix norms of **A** and **E** were also calculated to show the effect of the phase estimation error on the reconstruction.

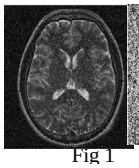

Fig 1

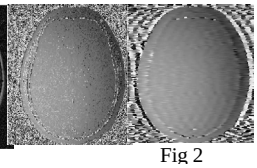

Fig 2

R=3 npe=85 | R=4,λ=1/8 npe=88 | R=4,λ=1/32 npe=70

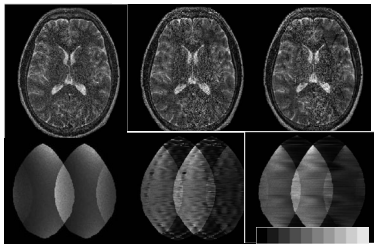

Fig.3 g 1 5 10

Results: Fig. 1 shows the magnitude and phase of the image. Fig. 2 shows a phase estimate at λ=1/8. The 2 leftmost images in fig. 3 show test 1, while the rightmost shows the (R=4, λ=1/32) experiment. Fig. 4 shows test 2. Fig. 5 shows the (R=5, λ=1/32) and (R=5, λ=1/2) simulations. g-factor maps accompany each of the SENSE or turboSENSE reconstructions. Furthermore, fig.6 shows a map of ||**E**||/||**A**|| for turboSENSE R=5 with the cases of λ=1/2 and λ=1/32.

R=4, npe=64 | R=5,λ=1/16 npe=64 | R=5,λ=1/32 npe=58 | R=5,λ=1/2 npe=154

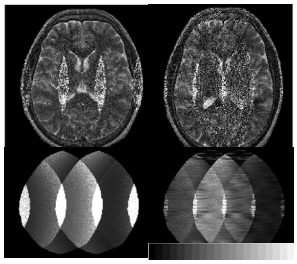

Fig.4 g 1 10 20

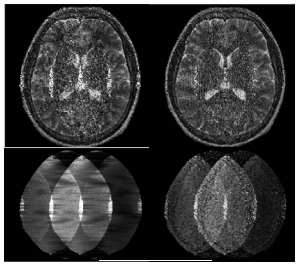

Fig.5

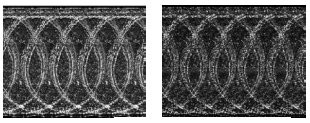

Fig.6

Discussion: Fig. 4 shows that SENSE R=4 performs inferior to turboSENSE R=5 because at a higher R when SENSE becomes ill-conditioned, turboSENSE is more robust to noise with smaller g-maps. Although turboSENSE utilizes a higher reduction factor than SENSE, it acquires more of the central k-space lines to obtain the phase estimate and behaves similarly to a variable density scheme. Fig. 5 shows that at λ=1/32, the quality has not decreased compared to λ=1/16. Thus, some net speedup can be gained by diminishing the resolution of the phase map without loss of image quality. The effects of phase estimation error can be seen in fig. 6, which shows the ||**E**||/||**A**|| values for the image at λ=1/32 and λ=1/2. Although the ||**E**||/||**A**|| decreases a little for λ=1/2 relative to λ=1/32, it is still significant at λ=1/2. The result is an improvement in image quality for λ=1/2, although the noise is still dominant at the edges. However, fig. 3 shows that SENSE R=3 is slightly visually better than turboSENSE R=4 at comparable number of phase encode steps. With turboSENSE R=4, decreasing the resolution of the phase map to λ=1/32 does not significantly degrade the image quality (see fig. 3 rightmost). The effects of the ringing from the low-resolution truncation can be seen in the resulting non-smooth g-maps. A g-map dependent filter can be used to remove some of this high frequency noise or to iteratively improve the reconstruction. Regularization can be used to further reduce the noise. Similar to partial k-space imaging, high-frequency phase transitions between water and lipids or pulsatile flow can impair high frequency components of the phase estimate, which thus propagates as residual aliasing into the reconstructed image. Another source of artifact may be from variable density EPI, when more phase is accrued from the traversal through the center of k-space at a lower velocity.

References: 1. Pruessman, K.P., et al. MRM, 42:952-962, 1999. 2. Bammer, R., PhD Thesis, Graz University of Technology, Graz, Austria, 2000. 3. Willig-Onwuachi, J.D., et al. Proceedings for the ISMRM 11th annual, 19, 2003. 4. Golub, G., Van Loan, C., Matrix Computations, The John Hopkins University, 1996.

Acknowledgments: Support was provided by GE Medical Systems, NIH grants RR09784, 1R01EB002771, 1R01NS35959, and GM08412, the Lucas Foundation, and the NIH Biotechnology-in-Training Fellowship.